Optimizing magnetically shielded solenoids for polarized ³He applications

W. C. Chen[1], Md. T. Hassan[1,2], R. Erwin[1], S. M. Watson[1], T. R. Gentile[1], G. L. Jones[3]

[1]National Institute of Standards and Technology, Gaithersburg, MD 20899, USA

[2]Department of Materials Science & Engineering, University of Maryland, College Park, Maryland 20742, USA

[3]Department of Physics, Hamilton College, Clinton, New York 13323, USA

Abstract

An important consideration when designing a magnetostatic cavity for polarized ³He applications is to minimize the transverse field gradient and maximize the ratio of the volume of field homogeneity to the overall size of the cavity. We report a design of a magnetically shielded solenoid (MSS) that significantly improves the transverse field gradient averaged over a volume of 1000 cm³ by placing compensation coils around the holes in the mu-metal end caps rather than the conventional design in which the compensation coils are placed on the main solenoid. Our application is polarized ³He-based neutron spin filters, and our goal was to minimize the volume-averaged transverse field gradient, thereby the gradient induced relaxation rate, over a ³He cell. For solenoids with end cap holes of different sizes, additional improvements in the field gradient were accomplished by introducing non-identical compensation coils centered around the non-identical holes in the end caps. The improved designs have yielded an overall factor of 7 decrease in the gradient in the solenoid, hence a factor of 50 increase in the gradient induced relaxation time of the ³He polarization. We present the results from both simulation and experiments for the development of several such solenoids. Whereas our focus is on the development of magnetically shielded solenoids for ³He neutron spin filters, the approach can be applied for other applications demanding a high level of field homogeneity over a large volume.

Magnetic field and gradient simulation

Simulations using the finite element software package RADIA and the Mathematic interface for analytical calculation of the field gradients were done for three different configurations of compensation coils, (1) identical compensation coils are placed on the solenoid at the ends, denoted as **end compensation**; (2) the compensation coils of the same diameter centered around the hole of each end cap, denoted as **identical hole compensation**; (3) the compensation coils matching to the different diameter holes in the end caps, denoted as **non-identical hole compensation**. Field homogeneity was significantly improved by placing the compensation coils only around the holes of the mu-metal end caps as shown below.

Normalized line-averaged gradients (NVATG) $|\partial B_z/z|/B$ and NVATGs were calculated as a function of the number of turns of the compensation coil for a cylindrical ³He cell 12 cm in diameter and 10 cm long for the hole compensation configurations. The normalized linear-averaged gradients (NLAG) minimizes at the same location as the NVATG. This shows that the NLAG can be used a direct evaluation criterion for minimizing the NVATG when experimentally optimizing a MSS.

NVATG is sensitive to the location of the compensation coil. Compensating the hole yields the lowest gradient.

Normalized Bz $|\partial B_z/z|/B\ cm^{-1}$

NVATG is 9.8x10⁻⁴ cm⁻¹ and 1.2x10⁻⁴ cm⁻¹ for the end compensation and identical hole compensation, respectively. This indicated an improvement in the NVATG by a factor of 8.2 for the identical hole compensation compared to the end compensation.

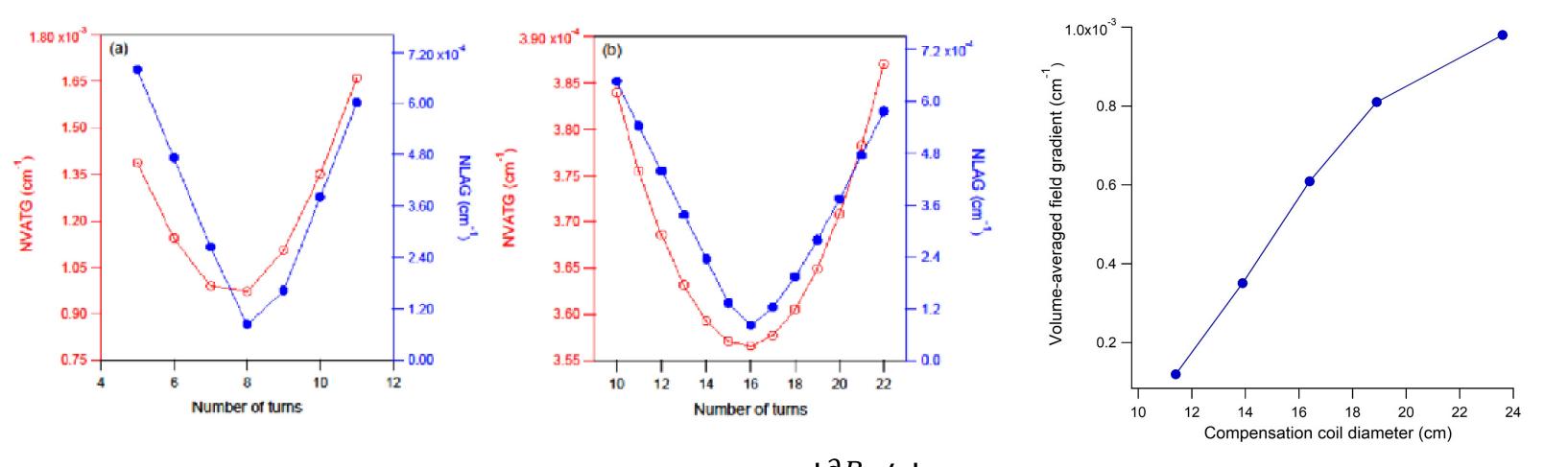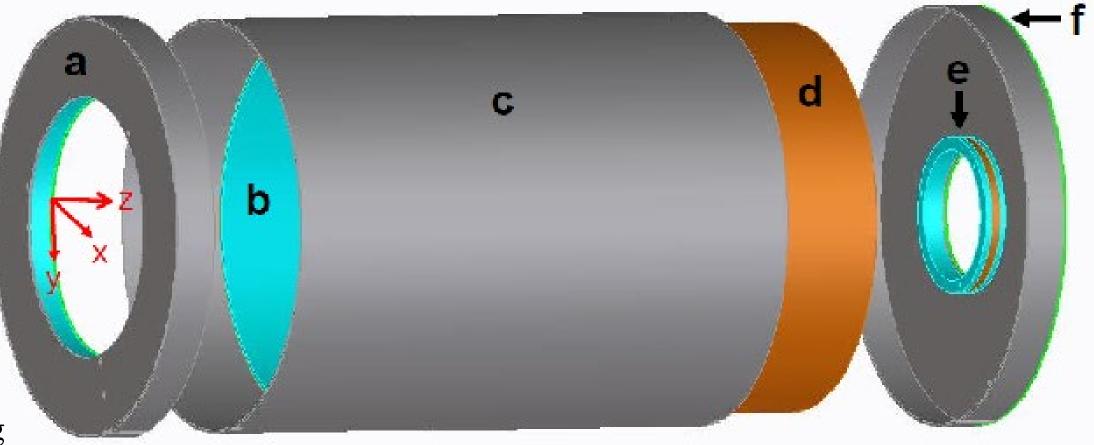## Design of magnetically shielded solenoids and field gradients

Relaxation time contributions:

(i) Dipole-dipole interactions, T_1^{dd}; (ii) Wall relaxation, T_1^w; (iii) Magnetic field gradients, T_1^{fg}

$$\frac{1}{T_1} = \frac{1}{T_1^{dd}} + \frac{1}{T_1^w} + \frac{1}{T_1^{fg}} \quad (1)$$

The normalized volume-averaged transverse field gradient (NVATG), $\frac{|\vec{\nabla}B_\perp|}{B}$, in cm⁻¹ over the cell volume V [1]:

$$\frac{1}{T_1^{fg}} = \frac{6700}{pV} \iiint \left(\frac{|\vec{\nabla}B_x|^2}{B^2} + \frac{|\vec{\nabla}B_y|^2}{B^2} \right) dx\,dy\,dz \equiv \frac{6700}{p}\left(\frac{|\vec{\nabla}B_\perp|}{B}\right)^2 h^{-1} \quad (2)$$

Design of a MSS:

Holes on the end caps for neutron beam path

a: Co-netic mu-metal end caps
b: Aluminum solenoid
c: Co-netic mu-metal cylinder
d: Copper winding
e: Compensation coils (this work)
f: Borated aluminum neutron shielding
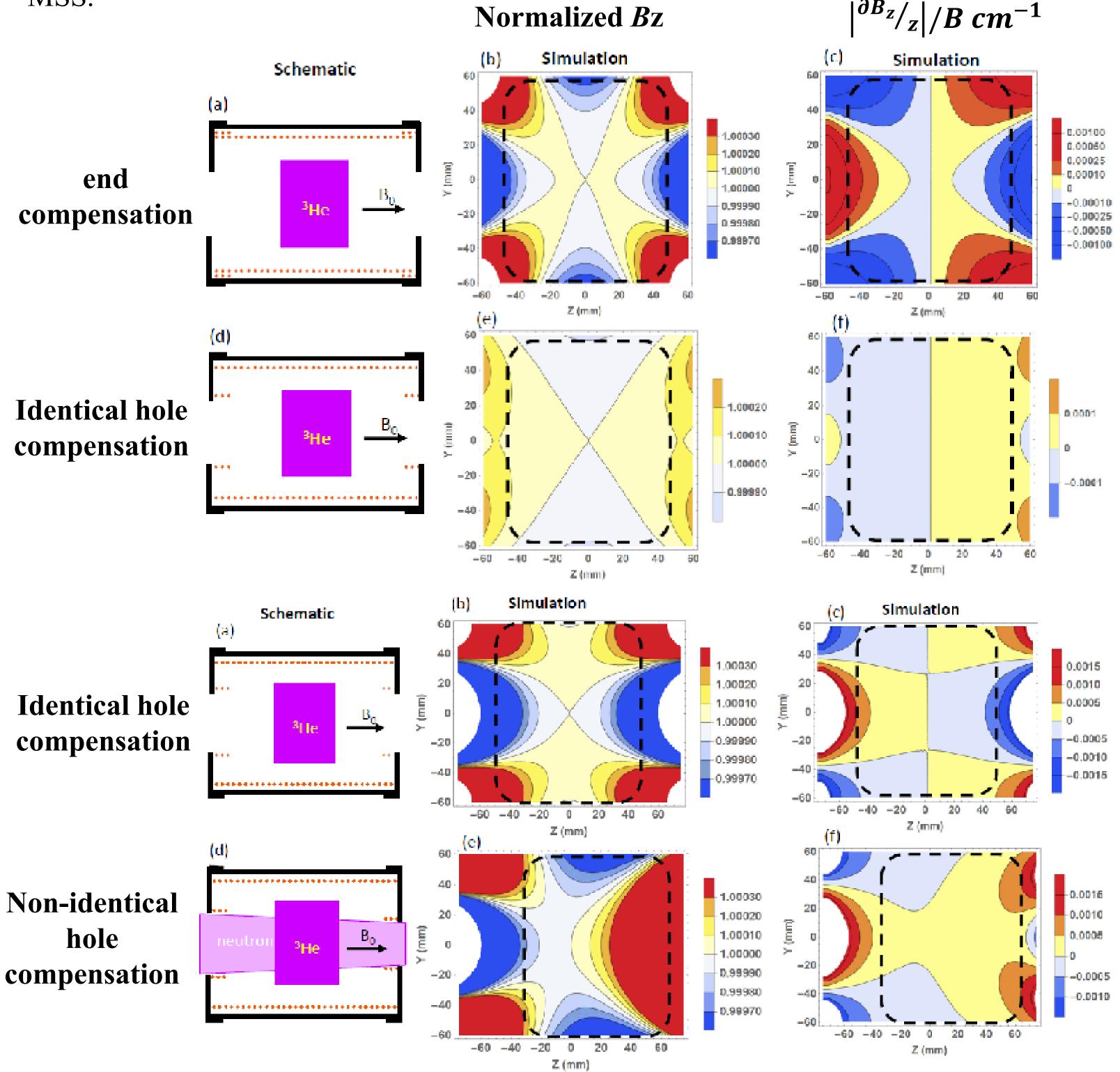

Results

Field gradient determination

Field gradient induced relaxation time T_1^{fg} was determined using Eq. 1 and a long combined T_1^{dd} and T_1^w relaxation time (longer than 450 h). NVATGs were then determined using Eq. 2.

Compensating the hole of the end cap

Compensation configuration	$\frac{|\vec{\nabla}B_\perp|}{B}$ 10⁻⁴ cm⁻¹	$\frac{|\vec{\nabla}B_\perp|}{B}^{cal}$ 10⁻⁴ cm⁻¹
End compensation	9.8 ± 0.2	9.8
Hole compensation	2.8 ± 0.1	1.2

The relaxation times of the cell Teroldego in the MSS Gemini were measured to be (145±4) h and (411±9) h for the end and hole compensation, respectively. The corresponding field gradients are (9.8±0.2)x10⁻⁴ cm⁻¹ and (2.8±0.2)x10⁻⁴ cm⁻¹, an improvement by a factor of 3.5.

Compensation with non-identical holes

Solenoid	Ø × ι (cm×cm)	d_s (cm)	d_l (cm)	T_1^e (h)	$\frac{|\vec{\nabla}B_\perp|}{B}$ (10⁻⁴ cm⁻¹)	$\frac{|\vec{\nabla}B_\perp|}{B}^{cal}$ (10⁻⁴ cm⁻¹)	$\frac{|\vec{\nabla}B_\perp|}{B}^{cal}_{sym}$ (10⁻⁴ cm⁻¹)
Honesty	27.9 × 35.6	11.7	14.3	415 ± 3	3.7 ± 0.2	3.5	4.8
Nyx	25.5 × 29.5	10.3	12.6	370 ± 8	4.2 ± 0.2	4.9	11.0
Venus	25.4 × 33.0	9.0	16.0	300 ± 10	4.4 ± 0.2	5.6	11.0

This table shows NVATGs for three MSSs for three different polarized neutron instruments. $\frac{|\vec{\nabla}B_\perp|}{B}^{cal}$ is the calculated NVATG at optimization of a MSS and $\frac{|\vec{\nabla}B_\perp|}{B}^{cal}_{sym}$ is the calculated NVATG at optimization with the larger compensation coil. The calculated gradients with the non-identical compensation configuration are up to a factor of 2.2 smaller than those with identical larger compensation coils. This implied an additional improvement in the gradient induced relaxation time by a factor of over 4.

Size of the homogeneous magnetic field region

Cavity type	Dimensions (cm × cm)	γ	$d_h \times l_h$ (cm×cm)	$\frac{|\vec{\nabla}B_\perp|}{B}$ (10⁻⁴ cm⁻¹)
Solenoid[2]	25.4×35.6	0.064	12×10	2.8 ± 0.1
Solenoid[2]	25.4×33	0.061	12×9	4.4 ± 0.2
Solenoid[2]	27.9×35.6	0.055	12×9	3.7 ± 0.2
Solenoid[2]	25.5×29.5	0.078	12×10	4.2 ± 0.2
Magic box[3]	40×15×28.4	0.066	12×10	5.7 ± 0.2
Solenoid[4]	27.2×36.4	0.037	10×10	<4.0
Magic box[5]	20×40×78	0.015	8×10	4.4
Magic box[6]	40×17×80	0.005	6×10	<2.0

To fit a cavity into a constrained space, it is necessary to maximize the homogeneous field region. Define γ to be the ratio of the volume of the most homogeneous field region to that occupied by the magnetic cavity. This tables summarizes a comparison of the value of γ from various designs of the magnetostatic cavities. d_h and l_h are the diameter and length of the cylinder of the homogenous field region. It is apparent that MSSs typically provide larger values of γ than magic boxes with the exception of end-compensated magic boxes.

Conclusions

- The conveniently measurable NLAG has been confirmed as a good indicator of NVATG.
- Placing the compensation coils centered around the hole of the end caps in a MSS yielded an improvement in the volume averaged transverse gradient by a factor of 3.5 over the conventional end compensation. This implies an improvement of a factor of 12 in the gradient induced relaxation time.
- An additional improvement in the gradient up to a factor of 2 was confirmed by implementing a non-identical compensation coil centered around the non-identical hole in the end cap.
- Several MSSs developed using this hole compensation approach yielded a significantly larger ratio of the volume of the homogenous field region to that of the device itself.

[1] G. D. Cates et al, Phys. Rev. A **37**, 2877 (1988); [2] W. C. Chen et al, Rev. Sci. Instrum. **91**, 105102 (2020).

[3] J. W. McIver et al, Rev. Sci. Instrum. **80**, 063905 (2009); [4] H. Kira et al, Phys. Procedia **42**, 200-205 (2013).

[5] E. Babcock et al, J. Phys. Conf. Ser. **1316**, 012019 (2019); [6] A. K. Petoukhov et al, Nucl. Instrum. Methods Phys. Rev. Sect. A **560**, 480 (2006).

Contact: wcchen@nist.gov